

A quantum transfer matrix method for one-dimensional disordered electronic systems

L P Yang¹, Y J Wang², W H Xu¹, M P Qin³ and T Xiang^{1,3}

¹ Institute of Theoretical Physics, Chinese Academy of Sciences, PO Box 2735, Beijing 100080, People's Republic of China

² Department of Physics, Beijing Normal University, Beijing 100875, People's Republic of China

³ Institute of Physics, Chinese Academy of Sciences, PO Box 603, Beijing 100080, People's Republic of China

Received 24 October 2008, in final form 24 February 2009

Published 13 March 2009

Online at stacks.iop.org/JPhysCM/21/145407

Abstract

We develop a novel quantum transfer matrix method to study thermodynamic properties of one-dimensional (1D) disordered electronic systems. It is shown that the partition function can be expressed as a product of 2×2 local transfer matrices. We demonstrate this method by applying it to the 1D disordered Anderson model. Thermodynamic quantities of this model are calculated and discussed.

(Some figures in this article are in colour only in the electronic version)

1. Introduction

For real solids, perfect periodicity is an idealization, while the imperfections are of great importance for transport properties. The broken translational symmetry makes the system deviate from the extended Bloch wave behavior, and in some cases, to localized states. As pointed out in [1], we cannot adopt the model of ordered systems to understand disordered materials. The concept of Anderson localization [2] and the correlation effect [3] among electrons in a disordered medium are two important ingredients in the understanding of disordered systems.

As a minimal Hamiltonian for independent electrons in a disordered potential, the Anderson disordered model remains difficult to understand at finite temperature. The disorder itself invalidates conventional analytical methods. No proper perturbation parameter can be chosen to deal with the disordered Hamiltonian although perturbation theory was applied to calculate the conductivity in the weak disorder limit. Considerable efforts focus on Anderson localization and the corresponding metal–insulator transition. In particular, a great insight was gained from scaling analysis [4, 5].

In contrast to higher dimensional cases, 1D models are often accessible to obtain detailed theoretical (analytical and numerical) results. However, in the disordered case, it is

intractable to make calculations in the thermodynamic limit by analytical methods even in 1D. The aim of this work is to develop a novel method to resolve this technical problem. Our method avoids direct diagonalization of the Hamiltonian and allows the thermodynamic limit to be explored directly and accurately. The key point lies in the fact that we can exploit the full translational symmetry in the Trotter (imaginary time or inverse temperature) direction after trading the evolution in the real space direction with the Trotter one.

It should be noted that the transfer matrix introduced in the present scheme is not the one usually used in the study of disordered systems [6]. Our starting point is to express the partition function of the system analytically in terms of the transfer matrix, rather than to use it to trace the eigenvalues or wavefunctions.

We will take the disordered Anderson model, as an example, to demonstrate how the quantum transfer matrix method works. The Hamiltonian is defined by

$$H = - \sum_i t_i (c_i^\dagger c_{i+1} + \text{h.c.}) + \sum_i (U_i - \mu) c_i^\dagger c_i, \quad (1)$$

where t_i is the hopping integral between two adjacent sites, $c_i (c_i^\dagger)$ is a fermion annihilation (creation) operator at site i , U_i is the diagonal disordered potential, and μ is the chemical potential. t_i and U_i can take random values satisfying their respective distributions.

2. Quantum transfer matrix method

As in the quantum transfer matrix renormalization group (TMRG) [7–9] method, we first separate H into two parts, $H = H_1 + H_2$, with each part a sum of commuting terms:

$$H_1 = \sum_{i=\text{odd}} h_{i,i+1}, \quad H_2 = \sum_{i=\text{even}} h_{i,i+1}, \quad (2)$$

where

$$h_{i,i+1} = -t_i(c_i^\dagger c_{i+1} + \text{h.c.}) + (U_i - \mu)n_i. \quad (3)$$

The TMRG uses the second-order approximation of the Trotter–Suzuki formula [10, 11]

$$Z = \text{Tr}(e^{-\beta H}) = \text{Tr}(V_1 V_2)^M + \text{O}(\epsilon^2), \quad (4)$$

where $\beta = 1/k_B T$ and T is the temperature. β is then divided into M parts uniformly, $\epsilon = \beta/M$ and M is the Trotter number. In the following discussions, we set $\epsilon = 0.01$ for high accuracy. The Trotter number M will increase with decreasing temperature. In our physical results the lowest temperature calculated is $T = 0.01$ ($k_B = 1$). Certainly, lower temperature results can be obtained if larger M is chosen. Considering the physical quantities, for example, the specific heat C is the second-order derivative of the free energy. Therefore, for $\epsilon = 0.01$, the results at $T \sim 0.001$ are still sound in the case of a system size $L > 10^5$.

$$V_1 = e^{-\epsilon H_1} = \prod_{i=\text{odd}} v_{i,i+1}, \quad (5)$$

$$V_2 = e^{-\epsilon H_2} = \prod_{i=\text{even}} v_{i,i+1},$$

where $v_{i,i+1}$ are the local evolution operators defined by $v_{i,i+1} = e^{-\epsilon h_{i,i+1}}$. By inserting $2M$ identities

$$\sum |n_1 \cdots n_N\rangle \langle n_1 \cdots n_N| = 1 \quad (6)$$

between the neighboring V_1 and V_2 operators in (4) and labeling successively the complete bases with $l \in [1, 2M]$ (so called imaginary time slices), the partition function can then be expressed as

$$Z = \lim_{\epsilon \rightarrow 0} \sum_{\{n_i^l\}} \prod_{l=1}^M \langle n_1^{2l-1} \cdots n_N^{2l-1} | V_1 | n_1^{2l} \cdots n_N^{2l} \rangle$$

$$\times \langle n_1^{2l} \cdots n_N^{2l} | V_2 | n_1^{2l+1} \cdots n_N^{2l+1} \rangle$$

$$= \lim_{\epsilon \rightarrow 0} \sum_{\{n_i^l\}} \prod_{l=1}^M (v_{1,2}^{2l-1,2l} \cdots v_{N-1,N}^{2l-1,2l})$$

$$\times (v_{2,3}^{2l,2l+1} \cdots v_{N,1}^{2l,2l+1}), \quad (7)$$

where $v_{i,i+1}^{l,l+1} = \langle n_i^l, n_{i+1}^l | v_{i,i+1} | n_i^{l+1}, n_{i+1}^{l+1} \rangle$ represents the matrix elements of $v_{i,i+1}$. The subscripts i and superscripts l for n and v stand for the coordinates in the real and Trotter directions, respectively. If we collect all $v_{i,i+1}^{l,l+1}$ with the same $(i, i+1)$, the partition function can be re-expressed as the column quantum transfer operators [11, 12]:

$$Z = \lim_{\epsilon \rightarrow 0} \text{Tr}\{T_{1,2} T_{2,3} \cdots T_{N,1}\}. \quad (8)$$

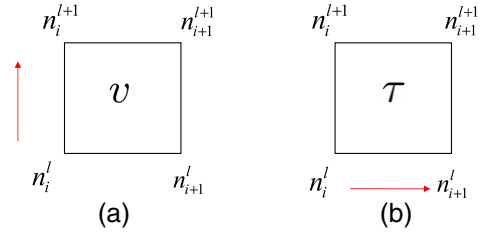


Figure 1. Graphical representation of the local evolution operator v (a) and the local transfer matrix (b) along the Trotter and real space directions, respectively.

In equation (8), there exist N site-dependent column transfer operators $T_{i,i+1}$, which are defined by a product of M local transfer operators,

$$T_{2i-1,2i} = \prod_l \tau_{2i-1,2i}^{2l-1,2l} \quad (9)$$

$$T_{2i,2i+1} = \prod_l \tau_{2i,2i+1}^{2l,2l+1},$$

where the matrix element of the local transfer operator τ is defined by

$$\tau_{i,i+1}^{l,l+1} \equiv \langle n_i^l, 1 - n_i^{l+1} | v_{i,i+1} | 1 - n_{i+1}^l, n_{i+1}^{l+1} \rangle. \quad (10)$$

The evolution of this matrix is illustrated in figure 1. The reason for labeling the basis state by $1 - n_i^l$ is to ensure the conservation of the total occupation number of two adjacent sites in the Trotter direction. Since $h_{i,i+1}$ conserves the total occupation number at sites i and $i+1$, subspaces $\{|1, 1\rangle\}$, $\{|0, 0\rangle\}$ and $\{|0, 1\rangle, |1, 0\rangle\}$ are decoupled. In writing equation (7), a periodic boundary condition $n_i^1 = n_i^{2M+1}$ is imposed in the Trotter direction.

Now let us introduce the following site-dependent variables:

$$\alpha_i = -\frac{\epsilon(U_i - \mu)}{2}, \quad \gamma_i = \sqrt{\alpha_i^2 + \epsilon^2 t_i^2},$$

$$b_i = e^{\alpha_i}, \quad u_i = \frac{\epsilon t_i \sinh \gamma_i}{\gamma_i}, \quad (11)$$

$$a_i = \cosh \gamma_i, \quad w_i = \frac{\alpha_i \sinh \gamma_i}{\gamma_i},$$

b_i and γ_i are defined by α_i , in addition, there is the expression $\cosh^2 \gamma_i - \sinh^2 \gamma_i = 1$. So, only three of six parameters are independent due to three related formulae. In terms of these variables, we obtain the following matrix elements for $v_{i,i+1}$ in the state number representation $\{|00\rangle, |01\rangle, |10\rangle, |11\rangle\}$:

$$v_{i,i+1}^{l,l+1} = b_i \begin{pmatrix} b_i^{-1} & 0 & 0 & 0 \\ 0 & a_i - w_i & u_i & 0 \\ 0 & u_i & a_i + w_i & 0 \\ 0 & 0 & 0 & b_i \end{pmatrix}. \quad (12)$$

According to the procedure mentioned above, the resulting local transfer matrix in the Trotter direction between slices l and $l+1$ is also block-diagonal because of fermion number

conservation. Consequently,

$$\tau_{i,i+1}^{l,l+1} = b_i \begin{pmatrix} u_i & 0 & 0 & 0 \\ 0 & a_i - w_i & b_i^{-1} & 0 \\ 0 & b_i & a_i + w_i & 0 \\ 0 & 0 & 0 & u_i \end{pmatrix}. \quad (13)$$

It can be shown that this transfer matrix has the following operator form:

$$\begin{aligned} \frac{\tau_{i,i+1}^{l,l+1}}{u_i b_i} &= 1 + \left(\frac{a_i}{u_i} - 1 \right) (d_l^\dagger d_l - d_{l+1}^\dagger d_{l+1})^2 + \frac{b_i}{u_i} d_l^\dagger d_{l+1} \\ &+ \frac{b_i^{-1}}{u_i} d_{l+1}^\dagger d_l + \frac{w_i}{u_i} (d_l^\dagger d_l - d_{l+1}^\dagger d_{l+1}), \end{aligned} \quad (14)$$

where the d 's are fermion operators defined in the Trotter space. $\tau_{i,i+1}^{l,l+1}$ is a quadratic function of fermion operators. Furthermore, $\tau_{i,i+1}^{l,l+1}$ can be exponentiated again to a concise quadratic form due to the fermion exclusion principle. For simplicity, we denote $C_i = u_i b_i$, $s_i \equiv \sqrt{p_i q_i + r_i^2}$, $n_l = d_l^\dagger d_l$ and

$$A = p_i d_l^\dagger d_{l+1} + q_i d_{l+1}^\dagger d_l + r_i (n_l - n_{l+1}), \quad (15)$$

then,

$$\begin{aligned} \frac{\tau_{i,i+1}^{l,l+1}}{C_i} &\equiv \exp[p_i d_l^\dagger d_{l+1} + q_i d_{l+1}^\dagger d_l + r_i (n_l - n_{l+1})] \\ &= 1 + (\cosh s_i - 1)(n_l - n_{l+1})^2 + \frac{\sinh s_i}{s_i} A. \end{aligned} \quad (16)$$

This exponential quadratic operator form of $\tau_{i,i+1}^{l,l+1}$ is valid only when the four coefficients before $(n_l - n_{l+1})^2$, $(n_l - n_{l+1})$, $d_l^\dagger d_{l+1}$, and $d_{l+1}^\dagger d_l$ satisfy the following four equations:

$$\begin{aligned} \cosh s_i &= \frac{a_i}{u_i}, & \frac{\sinh s_i}{s_i} p_i &= \frac{b_i}{u_i}, \\ \frac{\sinh s_i}{s_i} q_i &= \frac{b_i^{-1}}{u_i}, & \frac{\sinh s_i}{s_i} r_i &= \frac{w_i}{u_i}. \end{aligned} \quad (17)$$

Now we can cast the column transfer matrix $T_{2i,2i+1}$ defined by equation (9) into the following form:

$$T_{i,i+1} = C_i^M \exp \left[\sum_{l=1}^M p_i d_{2l}^\dagger d_{2l+1} + q_i d_{2l+1}^\dagger d_{2l} + r_i (n_{2l} - n_{2l+1}) \right]. \quad (18)$$

$T_{i,i+1}$ is translational invariant in the Trotter direction. Therefore, we can introduce a Fourier transformation along this direction:

$$d_\omega = \begin{pmatrix} d_{\omega,1} \\ d_{\omega,2} \end{pmatrix} = \frac{1}{\sqrt{M}} \sum_{l=1}^M e^{-i\omega R_l} \begin{pmatrix} d_{2l-1} \\ d_{2l} \end{pmatrix}. \quad (19)$$

The general column transfer matrix can then be rewritten as

$$\begin{aligned} T_{2i-1,2i} &= C_{2i-1}^M \exp \left[\sum_{\omega} d_\omega^\dagger \begin{pmatrix} r_{2i-1} & p_{2i-1} \\ q_{2i-1} & -r_{2i-1} \end{pmatrix} d_\omega \right], \\ T_{2i,2i+1} &= C_{2i}^M \exp \left[\sum_{\omega} d_\omega^\dagger \begin{pmatrix} -r_{2i} & e^{-i\omega} q_{2i} \\ e^{i\omega} p_{2i} & r_{2i} \end{pmatrix} d_\omega \right]. \end{aligned} \quad (20)$$

Substituting these transfer matrices into equation (8), we obtain the following expression for the partition function:

$$Z = \prod_i C_i^M \prod_{\omega} \text{Tr}[2 + T_\omega], \quad (21)$$

where

$$T_\omega = \prod_{i=1}^{N/2} t_{2i-1} t_{2i,\omega}, \quad (22)$$

t_{2i-1} and $t_{2i,\omega}$ are 2×2 matrices defined by

$$\begin{aligned} t_{2i-1} &= \frac{1}{u_{2i-1}} \begin{pmatrix} a_{2i-1} - w_{2i-1} & b_{2i-1}^{-1} \\ b_{2i-1} & a_{2i-1} + w_{2i-1} \end{pmatrix}, \\ t_{2i,\omega} &= \frac{1}{u_{2i}} \begin{pmatrix} a_{2i} + w_{2i} & e^{-i\omega} b_{2i} \\ e^{i\omega} b_{2i}^{-1} & a_{2i} - w_{2i} \end{pmatrix}. \end{aligned} \quad (23)$$

In obtaining these expressions, we have used the fact that $\tau_{i,i+1}^{l,l+1}/C_i$ is an identity matrix in the subspace $\{|1, 1\rangle, |0, 0\rangle\}$. In equation (22), all multiplied matrices are exponential of traceless matrices. Thus the eigenvalue of the final matrix after multiplications will have the form $\exp[\pm\lambda(\omega)]$. In the thermodynamic limit, the larger eigenvalue $\exp[\lambda(\omega)]$ (assuming $\lambda(\omega)$ is positive) will become even larger during the multiplication in equation (22), hence the constant 2 in equation (22) can be neglected because the eigenvalue $\exp[\lambda(\omega)]$ dominates.

It should be noted that ω is related to the parity of M . For odd M

$$\omega = \frac{2m\pi}{M}, \quad m = -\frac{M-1}{2}, \dots, 0, \dots, \frac{M-1}{2}, \quad (24)$$

and for even M

$$\omega = \frac{(2m+1)\pi}{M}, \quad m = -\frac{M}{2}, \dots, -1, 0, \dots, \frac{M}{2} - 1. \quad (25)$$

The transfer matrix T_ω in equation (22) is calculated in the subspace of $\{|0, 1\rangle, |1, 0\rangle\}$, so the fermion occupation number is 1 for each two unit cells along the Trotter direction. The state space for one column transfer matrix is

$$d_1^\dagger d_2^\dagger \cdots d_{2M-1}^\dagger d_{2M}^\dagger |0\rangle \quad (26)$$

and the total occupation number is M . Due to the periodicity in Trotter direction, it is equivalent to calculating, in the state space,

$$d_2^\dagger d_3^\dagger \cdots d_{2M}^\dagger d_{2M+1}^\dagger |0\rangle. \quad (27)$$

However, permuting the fermion operator d_1^\dagger behind d_{2M}^\dagger will introduce a factor $(-1)^{M-1}$ because of the transposition with $(M-1)$ occupied fermions. Therefore, there is the relation,

$$(-1)^{M-1} d_1^\dagger = d_{2M+1}^\dagger. \quad (28)$$

For odd M , $d_1^\dagger = d_{2M+1}^\dagger$; for even M , $d_1^\dagger = -d_{2M+1}^\dagger$. As a result, ω takes values according to the formulae (24) and (25) respectively. In the following, we will set M even and use equation (25).

For the focused quantum transfer matrix (QTM) method, we emphasize that it can handle any one-dimensional site- or bond-independent fermion model without interaction.

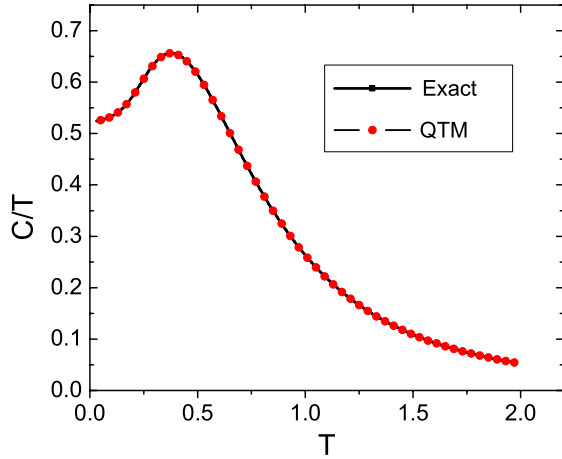


Figure 2. Comparison of the specific heat coefficient C/T obtained from two different methods: the exact energy spectrum calculation and the quantum transfer matrix method. Here, $t = 1$ and $U = 0$.

Certainly, any spin systems which can be transformed into the corresponding fermion models are included in the scope of the method's application. As shown in [13], T_ω in equation (22) can be formally regarded as the transfer matrix for the following 1D Ising model in a magnetic field:

$$Z = \sum_{S_i} \exp \left\{ \sum_i [J_i (S_i S_{i+1} - 1) + h_i S_i + f_i] \right\}. \quad (29)$$

For the odd sites, the parameters are ω -independent in the corresponding 1D Ising model with the relations

$$f_{2i-1} = -\frac{1}{2} (\ln |b_{2i-1}|), \quad (30)$$

$$h_{2i-1} = \ln \frac{(a_{2i-1} - w_{2i-1})}{(b_{2i-1} + w_{2i-1})}, \quad (31)$$

$$J_{2i-1} = \frac{1}{4} \ln \frac{2u_{2i-1}}{|b_{2i-1}|}. \quad (32)$$

However, the situation is different for even sites and the parameters J_i, f_i are now ω -dependent

$$f_{2i} = \frac{1}{2} (\ln |b_{2i}| + i\omega), \quad (33)$$

$$h_{2i} = \ln \frac{(a_{2i} + w_{2i})}{(a_{2i} - w_{2i})}, \quad (34)$$

$$J_{2i} = \frac{1}{4} (2 \ln(u_{2i} |b_{2i}|) + i\omega). \quad (35)$$

The correspondence for even sites cannot provide a material mapping to 1D Ising model because of the complex parameters, which arise from the Fourier transformation along the Trotter direction. Since there exists a relation $T_\omega^* = T_{-\omega}$, due to the factor $e^{i\omega}$, we can multiply in pairs the transfer matrices with ω and $-\omega$. In fact, the pairwise multiplication can save us half of the calculation because of the complex conjugate relation. When using equation (22) to solve the partition function, what is needed is to calculate the product of N matrices of dimension 2 for a given ω . Once Z is obtained, the calculation of the free energy is direct, $F = -T \ln Z$

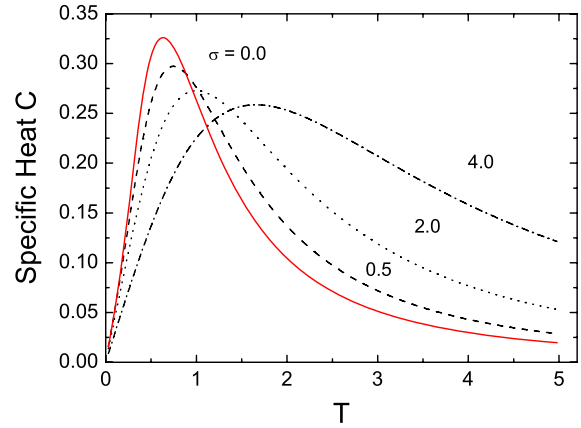


Figure 3. The specific heat C as a function of T for $\sigma = 0.5, 2, 4$, and 0 (red solid line).

(hereafter taking $k_B = 1$), from which all the other thermodynamic quantities of interest, such as the specific heat C , can be obtained.

Figure 2 shows the result of this comparison for the linear coefficient of the specific heat C/T . It is obvious that the two sets of data coincide completely. The chain length N , here, and in the rest of the paper is taken up to 2^{17} ($=131072$). Furstenburg's theorem [14] assures us that the partition function is independent of the sample when the system size is large enough. We need not take the random number average for disordered cases.

3. Results

3.1. Gaussian diagonal disorder

We first consider a Gaussian-like function

$$P(x) = \frac{1}{\sqrt{2\pi}\sigma} e^{-\frac{(x-a)^2}{2\sigma^2}} \quad (36)$$

for the disordered distribution of the diagonal potential U_i , where a and σ are the mean value and the standard deviation respectively. In the following discussion, we take $t = 1, a = 0, \mu = 0$. The controlling parameter is the standard deviation σ , which denotes the disorder degree of the distribution of U_i . In these figures, the red solid line means the case without disorder, i.e. $U_i = 0$ ($\sigma = 0$), and the other curves are for $\langle U_i \rangle = a = 0$ and $\sigma \neq 0$.

As shown in figures 3–5, the difference of the physical quantities is slight between the cases of $\sigma = 0.5$ and 0. However, significant differences appear when σ increases. With increasing σ , the peaks of the specific heat C move towards higher temperatures. The introduction of disordered diagonal energy widens the energy band. The density of states (DOS) distributes in a broaden energy range. This leads to the shift of the peak position of C towards higher temperature with increasing σ . The disorder assists the thermal fluctuations and shifts the peak of C/T to lower temperatures. The specific heat coefficient C/T at zero temperature is proportional to the

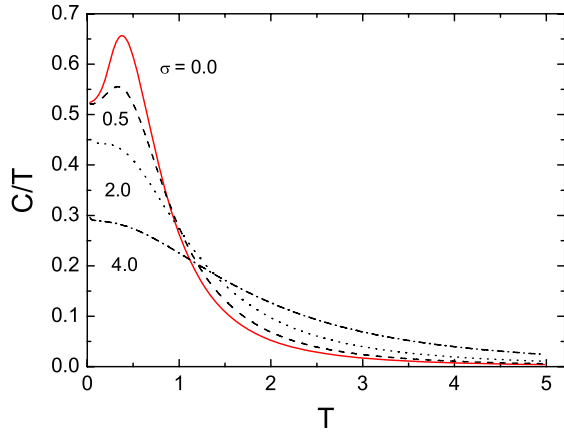


Figure 4. The specific heat coefficient C/T as a function of T for $\sigma = 0.5, 2, 4$, and 0 (red solid line).

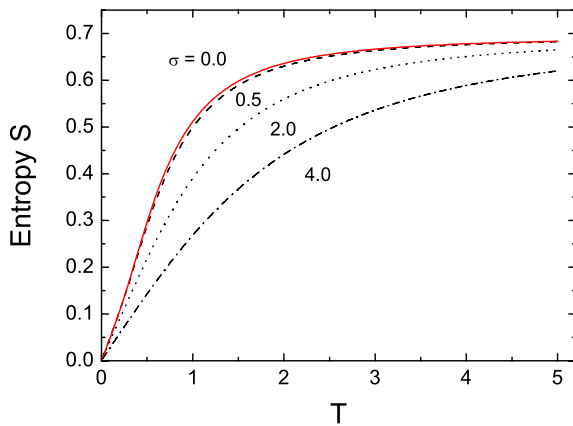


Figure 5. The entropy S as a function of T for $\sigma = 0.5, 2, 4$, and 0 (red solid line).

density of states around the Fermi energy E_F , i.e.,

$$\frac{C}{T} \Big|_{T \rightarrow 0} \propto \rho(E_F). \quad (37)$$

Figure 4 shows that when the disorder increases, the density of states near the Fermi surface decreases. The entropy S decreases when σ increases.

Figure 6 shows how the chemical potential μ changes with T for some given occupation numbers N . N becomes larger with increasing μ for fixed T , while N becomes smaller with increasing T for fixed μ . To keep N invariant, μ is a monotonic increasing function of T . The function shows a linear form in the high temperature regime.

In equation (21), the partition function is expressed as product of different ω components, consequently, the free energy F can be written as a sum of dependent free energy $F(\omega)$. For a given temperature T , $F(\omega)$ decreases with ω increasing. When the disorder is turned on, $F(\omega)$ changes little except in the vicinity of $\omega \sim \pi$. This can be seen from figure 7, which compares the difference of free energies between the disordered ($\sigma = 2$) and ordered cases as a function of ω . It clearly shows that the difference becomes significant

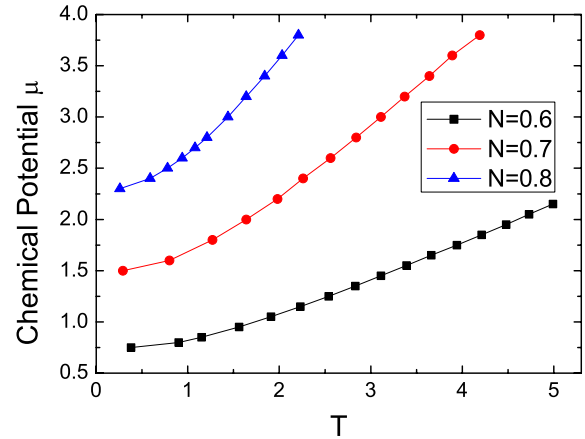


Figure 6. The chemical potential μ as a function of T for some fixed occupation numbers $N = 0.6, 0.7, 0.8$. $a = 0, \sigma = 2$, and $t = 1$.

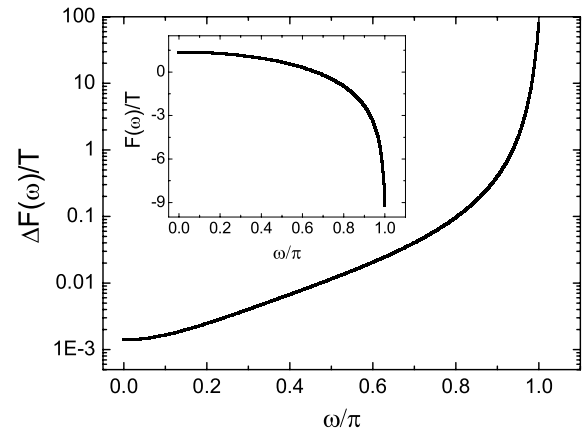


Figure 7. The difference $\Delta F(\omega)/T$ between disordered and uniform cases as a function of ω/π . Here, $T = 0.01, t = U = 1, \sigma = 2$. The inset shows the ω dependence of $F(\omega)/T$ for the system without disorder.

only when ω approaches π . In [13], the singularity from some special ω 's was used to discuss the phase transition.

3.2. Staggered disorder potential

We now consider a special model whose diagonal potential energy is alternating (staggered) with the lattice site, i.e.,

$$t_i = t, \quad U_i = (-1)^i U + \Delta U_i. \quad (38)$$

When $\Delta U_i = 0$, the energy spectrum is readily calculated via the Fourier transformation,

$$c_i = \sum_k e^{iki} c_k, \quad c_i^\dagger = \sum_k e^{-iki} c_k^\dagger. \quad (39)$$

The result is a two sub-bands dispersion relation,

$$E_\pm = -2\mu \pm \sqrt{U^2 + 4t^2 \cos^2 k}. \quad (40)$$

The band gap is $2U$.

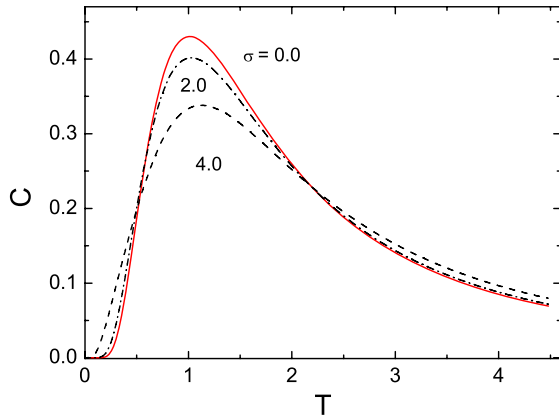


Figure 8. The specific heat C as a function of T for the uniform ($\sigma = 0$) and disordered ($\sigma = 2, 4$) potentials. $t = 1, U = 2, \mu = 0$.

Let us choose a uniform rectangular distribution $P(x) = \frac{1}{\sigma}$ for the increment of the random diagonal energy ΔU_i . Here, σ is the width of the rectangular distribution satisfying

$$P(x) = \begin{cases} \frac{1}{\sigma}, & \text{if } -\frac{\sigma}{2} \leq x \leq \frac{\sigma}{2}, \\ 0, & \text{otherwise.} \end{cases} \quad (41)$$

In the presence of disorder, the band gap is expected to decrease with an increase of the disorder degree σ . For small σ , there is a finite excitation gap and the specific heat drops exponentially at low temperature, as shown in figure 8.

We also consider the case when the random potential take only two discrete values: $-\sigma/2, \sigma/2$ with equal probability. We call it the discrete distribution of the increment, and the above rectangular distribution is denoted as the continuous one.

Figure 9 compares the specific heat coefficient C/T at $T = 0.01$ for the above two kinds of distribution of random potentials. In the case of the discrete distribution, C/T exhibits a sharper peak. When the disordered level σ increases to approximately 4, the band gap disappears. With a further increase in σ , C drops to zero because the band gap opens again for the discrete random potential. This can be understood as follows. The two sub-bands close with each other when disorder is introduced. The upper sub-band shifts downwards by $\sigma/2$ and the lower sub-band shifts upwards by $\sigma/2$. When the top of the original upper sub-band touches the zero energy, i.e., $\sigma/2 = 2\sqrt{2}$, the two sub-bands begin to separate again. Therefore, C/T decreases to zero at $\sigma \simeq 4\sqrt{2}$ in figure 9. On the contrary, for the continuous random increment case, C/T remains a finite value even for large σ . This is because the split of the upper and lower bands only expands the width of these two bands, and once they touch each other, they never separate again.

As a further investigation for C in the discrete distribution, we choose three typical disordered degrees $\sigma = 3.0, 4.8, 7.0$, corresponding to the three regions in figure 9, to show how C varies with the temperature at low T . As shown in figure 10, when $\sigma = 3.0$ and 7.0 , C drops exponentially with temperature at low temperatures. The double-peak structure of C can be understood from the overlaps of energy bands. The discrete

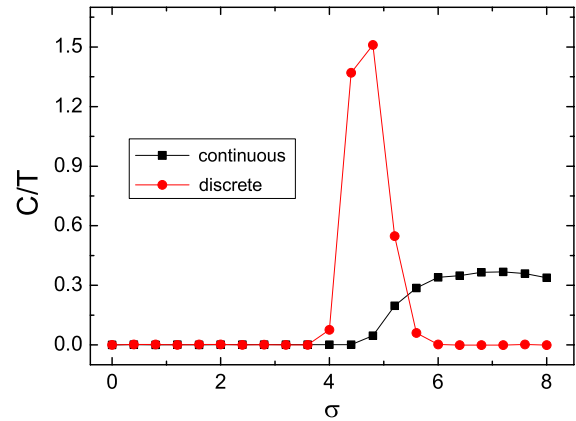


Figure 9. Comparison of the specific heat coefficient C/T for a continuous distributed random potential with that for a discrete random potential. $t = 1, U = 2, \mu = 0$ and $T = 0.01$.

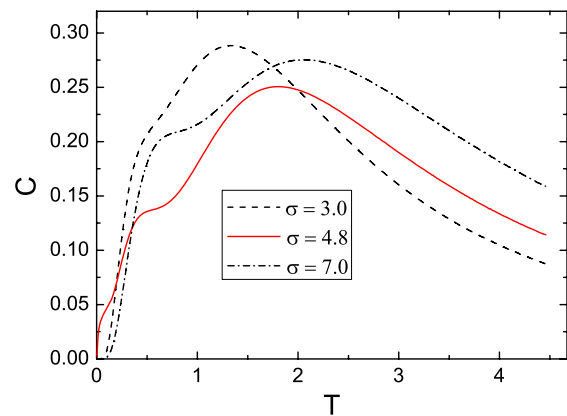


Figure 10. Temperature dependence of the specific heat in three different random potentials ($\sigma = 3.0, 4.8, 7.0$). $t = 1, U = 2, \mu = 0$.

increments split the original single energy band into two bands which shift upwards and downwards by $\sigma/2$. The resulting four bands from the upper and lower sub-bands meet pairwise. The thermal fluctuations cause the double peaks shown in C curves.

4. Conclusion

For the 1D disordered system, the quantum transfer matrix method we have developed is applicable to all kinds of disorder distribution types and strengths. The non-diagonal disordered problem can be handled, since the partition function Z can be expressed as the product of site-dependent local transfer matrices. Compared to the diagonal disordered cases, we only need to modify the local transfer matrix elements correspondingly.

We have studied the thermodynamic properties of the 1D disordered Anderson model. We discussed two kinds of diagonal (potential) disordered models, with or without staggered potentials. The free energy F can be written as a sum of different ω components from the Fourier transformation in Trotter space. Compared to the system without disorder, the

most significant difference in $F(\omega)$ shows only in the region very close to $\omega = \pi$. The disorder changes the distribution of DOS, leading to a difference in the thermodynamic quantities in comparison with the disorder-free system. All the results shown in the figures are for systems with a number of sites greater than 10^5 . This kind of calculation is far beyond the capacity of exact diagonalization.

The transfer matrix method has a broad range of applicability and can be used to discuss any non-interacting fermion model. Recently this method has been used to calculate the thermodynamic quantities of the Hofstadter model, which describes the behaviors of tightly-bound Bloch electrons in a magnetic field [15, 16]. In the Landau gauge, the Hofstadter Hamiltonian can be decoupled into a sum of one-dimensional Hamiltonians; this falls into the application range of the quantum transfer matrix method.

Acknowledgments

This work was supported by the National Natural Science Foundation of China and the National Program for Basic Research of MOST, China.

References

- [1] Lee P A and Ramakrishnan T V 1985 *Rev. Mod. Phys.* **57** 287
- [2] Anderson P W 1958 *Phys. Rev.* **109** 1492
- [3] Altshuler B L and Aronov A G 1979 *Solid State Commun.* **39** 115
- [4] Wegner F 1976 *Z. Phys. B* **25** 327
- [5] Abrahams E, Anderson P W, Licciardello D C and Ramakrishnan T V 1979 *Phys. Rev. Lett.* **42** 673
- [6] Brandes T and Kettemann S 2003 *Anderson Localization and its Ramifications* (Berlin: Springer)
- [7] Bursill R J, Xiang T and Gehring G A 1996 *J. Phys.: Condens. Matter* **8** L583
- [8] Wang X Q and Xiang T 1997 *Phys. Rev. B* **56** 5061
- [9] Xiang T and Wang X 1999 *Density-Matrix Renormalization: a New Numerical Method in Physics* ed I Peschel, X Wang, M Kaulke and K Hallberg (New York: Springer) pp 149–72
- [10] Trotter H F 1959 *Proc. Am. Math. Soc.* **10** 545
- [11] Suzuki M 1976 *Prog. Theor. Phys.* **56** 1454
- [12] Betsuyaku H 1985 *Prog. Theor. Phys.* **73** 320
- [13] Shankar R and Murthy G 1987 *Phys. Rev. B* **36** 536
- [14] Furstenberg H 1963 *Trans. Am. Math. Soc.* **108** 377
- [15] Xu W H, Yang L P, Qin M P and Xiang T 2008 *Phys. Rev. B* **78** 241102(R)
- [16] Yang L P and Xiang T 2009 unpublished